RUSSIAN SYNTHETIC AMETRINE

By Vladimir S. Balitsky, Taijin Lu, George R. Rossman, Irina B. Makhina, Anatolii A. Mar'in, James E. Shigley, Shane Elen, and Boris A. Dorogovin

Gem-quality synthetic ametrine has been produced commercially in Russia since 1994, by hydrothermal growth from alkaline solutions. Faceted synthetic ametrine has many similarities to its natural counterpart from Bolivia. For the most part, however, the synthetic ametrine obtained for this study could be identified by a combination of characteristics, including growth features such as twinning and color zoning. EDXRF chemical analyses revealed higher concentrations of K, Mn, Fe, and Zn than in natural ametrine. IR spectra of the synthetic citrine portions showed more intense absorption in the 3700–2500 cm^{-1} range compared to natural ametrine; the synthetic amethyst zones showed a weak diagnostic peak at 3543 cm^{-1}.

ABOUT THE AUTHORS

Dr. Balitsky (balvlad@iem.ac.ru) is head of the Laboratory of Synthesis and Modification of Minerals at the Institute of Experimental Mineralogy, Russian Academy of Science (IEM RAS), in Chernogolovka, Moscow District, Russia. Dr. Lu is a research scientist, Dr. Shigley is director, and Mr. Elen is a research gemologist at GIA Research, Carlsbad, California. Dr. Rossman is professor of mineralogy at the California Institute of Technology (Caltech) in Pasadena, California. Dr. Makhina is project leader, Dr. Mar'in is head of the Department for Experimental Mineralogy, and Dr. Dorogovin is a director at the Russian Research Institute for Material Synthesis (VNIISIMS) in Alexandrov, Vladimir District, Russia.

Please see acknowledgments at the end of the article.

Gems & Gemology, *Vol. 35, No. 2, pp. 122–134*

Amethyst is one of the most popular colored gemstones because of its color, availability, and affordability. Citrine is less often encountered in nature, although large quantities are produced by the heat treatment of amethyst. In the 1970s a spectacular combination of amethyst and citrine, commonly referred to as ametrine, became available (Hehar, 1980; Koivula, 1980; Vargas and Vargas, 1980). Although there was early speculation (stimulated in part by observations of Nassau, 1981) that such ametrine was synthetic or the effect was produced by treatment, the source of natural, untreated ametrine was eventually revealed to be the Anahí mine in Bolivia (Jones, 1993; Vasconcelos et al., 1994). In fact, efforts were underway in Russia in 1977 to understand the fundamental mechanisms of synthesizing ametrine (Balitsky and Balitskaya, 1986). By 1994, the growth technology was successfully established, and the first commercial batch (on the order of 100 kg) of synthetic ametrine crystals was produced.

Currently, a few kilograms per month of synthetic ametrine crystals and polished slabs are being sold. Faceted synthetic ametrine is also available (see, e.g., figure 1). Batch capacity has now grown to more than 300 kg. If necessary to meet demand, several tons of synthetic ametrine a year could be produced by a single laboratory (the Russian Research Institute for Material Synthesis [VNIISIMS] of the Ministry of Geology of the Russian Federation, in Alexandrov, Vladimir District). Most of the synthetic ametrine is sold in Russia. Recently, however, synthetic ametrine (of unknown origin) has appeared in the Bolivian market (Rivero, 1999).

Although at least three morphological types of synthetic ametrine crystals can be grown, this article reports on the most abundant commercial type. The cause of color, growth conditions, crystal morphology, gemological properties, internal features, spectra, and chemical composition are described, and key tests to separate this synthetic ametrine from its natural counterpart are summarized.

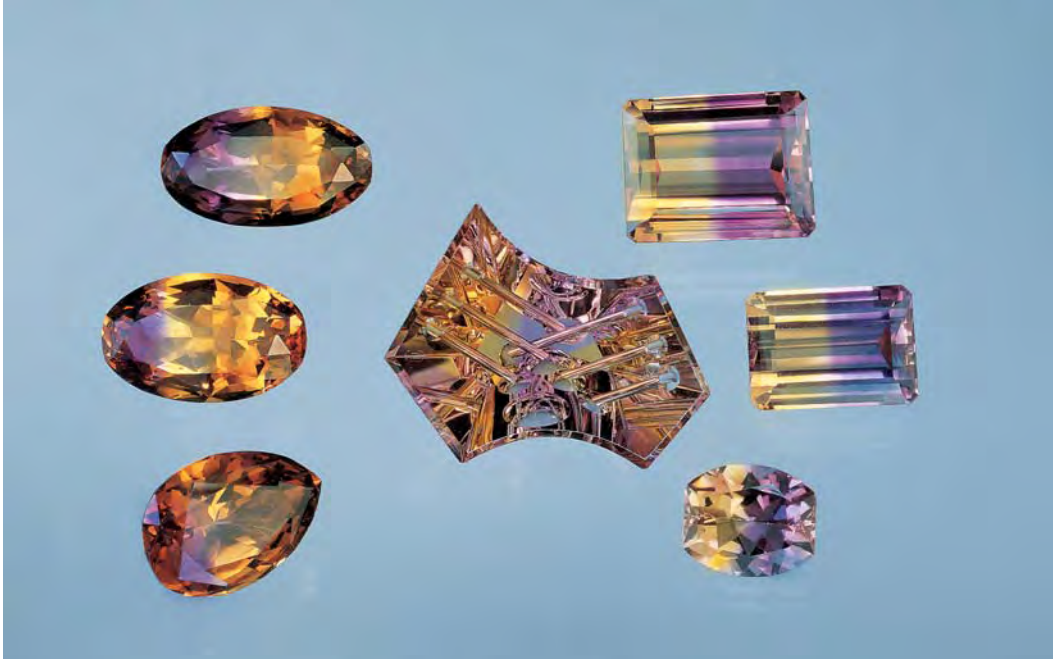

Figure 1. Synthetic ametrine hydrothermally grown in Russia became commercially available in the mid-1990s. Here, faceted synthetic ametrine (the three samples on the left, 11.30–13.38 ct) is shown together with natural ametrine from the Anahí mine in Bolivia. The carving of natural ametrine in the center weighs 35.15 ct and was executed by Michael Dyber; the faceted stones on the right weigh 4.71–22.31 ct. Photo © Harold & Erica Van Pelt.

HISTORICAL BACKGROUND

Synthetic quartz with the distinctive amethyst-citrine bi-coloration was first mentioned in the Russian scientific literature in the late 1950s and early 1960s. In particular, Tsinober and Chentsova (1959) reported that, after X-ray irradiation, certain crystals of brown synthetic quartz developed purple (amethyst) coloring in the rhombohedral growth sectors. This treatment phenomenon was revisited in the course of research into synthetic brown quartz and synthetic amethyst (e.g., Balakirev et al., 1979; Balitsky, 1980; Balitsky and Lisitsina, 1981; Nassau, 1981).

The first investigations aimed at producing synthetic ametrine on a commercial scale began in 1982 at the Institute of Experimental Mineralogy of the Russian Academy of Science (IEM RAS) in Chernogolovka, Moscow District. These experiments investigated how physical, chemical, and growth factors affected the capture and distribution of color-causing iron impurities during the growth of synthetic ametrine (as well as other iron-bearing varieties of quartz; see Balitsky and Balitskaya, 1986). In 1993–1994, the research was transferred to VNIISIMS, also near Moscow, although colleagues at both institutions continued to collaborate. Later, VNIISIMS organized a special company named "Аметрин" (Ametrine) to market synthetic ametrine. Today, almost all synthetic ametrine is produced at VNIISIMS.

SCIENTIFIC FOUNDATIONS FOR THE GROWTH OF SYNTHETIC AMETRINE

Iron Impurities in Colored Quartz. As previously established by several researchers (e.g., Hutton, 1964; Zaitov et al., 1974; Lehmann, 1975; Balakirev et al., 1979; Balitsky, 1980; and Rossman, 1994), the various colors of iron-bearing quartz (e.g., amethyst, citrine, green, and brown quartz) are related to different forms of iron (Fe) in the crystal structure. Only a small quantity of iron (e.g., about 0.01–0.05 wt.% Fe for amethyst) is needed to produce coloration in quartz. Even though the element iron and the mineral quartz are both common in nature, the occurrence of ametrine is quite rare. This is due to the specific physical, chemical, and geological conditions necessary for ametrine formation (Balitsky and Balitskaya, 1986; Vasconcelos et al., 1994).

The basic unit of the quartz structure is a tetrahedron consisting of a silicon (Si) atom and four oxygen (O) atoms. Trivalent iron (Fe^{3+}) can substitute for Si^{4+} in a tetrahedral site, or it can fill interstitial sites (as extra atoms in voids) between neighboring tetrahedra. At least two different interstitial positions exist in the quartz structure (Rossman, 1994, p. 434).

The amethyst coloration develops in a two-step process. First, the substitution of Si^{4+} by Fe^{3+} during growth produces a precursor center (Fe^{3+} substitutional center, $[FeO_4]^-$). The resulting deficiency of positive charge is compensated by the introduction of alkali metal ions (such as Li^+ or Na^+) or protons (H^+) into the quartz. This precursor center absorbs so little light that the material is almost colorless. The purple color develops only when the precursor center is converted to the amethyst color center ($[FeO_4]^0$) by exposure to ionizing radiation. For synthetic amethyst, a dose of 5–6 Mrads of cobalt-60 gamma-ray radiation is commonly used, although electron irradiation is employed occasionally.

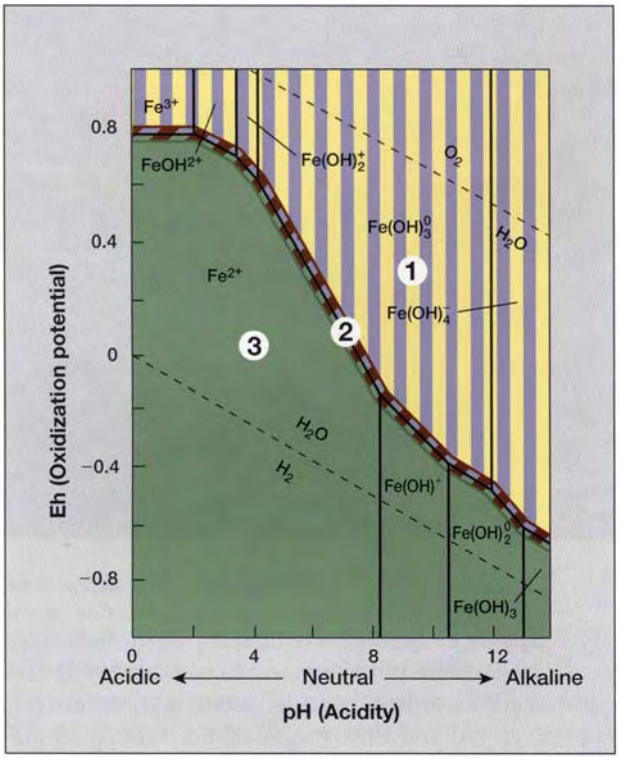

Figure 2. This diagram relates the Eh (oxidation potential) and pH (acidity) of iron (Fe)-containing aqueous solutions to the chemical form in which the iron exists in the solution. The regions corresponding to the various color varieties of iron-containing quartz are indicated by purple (amethyst), yellow (citrine), brown (brown quartz), and green (green quartz). 1 = region of amethyst, citrine, and ametrine (purple-and-yellow striped) formation; 2 = narrow region of brown quartz formation (along line), with adjacent green-and-brown quartz and amethyst-and-brown quartz regions; and 3 = region of green quartz formation. After Melnik et al. (1974).

Citrine coloration in synthetic quartz is also related to Fe^{3+}. However, in contrast to the color mechanism for amethyst, the iron does not enter the crystal structure. Rather, it is captured on growth faces of the quartz crystal—possibly as a small aggregate of a hydrated iron hydroxide—in the form of a so-called "nonstructural" impurity. Various colors can result, depending on the oxidation state (valence) of the nonstructural iron: Green coloration is caused by the presence of Fe^{2+} impurities, and the simultaneous capture of both Fe^{2+} and Fe^{3+} gives rise to brown quartz.

Because the color of iron-bearing quartz depends on the valence state of the iron, the Russian researchers first had to determine the conditions under which the desired form of iron ions would exist in the quartz-forming hydrothermal solutions. They did this with the help of a calculated diagram (known as an Eh-pH diagram—see e.g., Garrels and Christ, 1965; figure 2), which shows the stability of ionic and molecular forms of iron in aqueous solution as a function of the oxidation potential (Eh) and the acidity (pH). From this diagram, it can be seen that there is a limited regime under which all the iron will be in the trivalent state (i.e., region 1 in figure 2). This observation was fundamental to the development of technologies for growing both synthetic amethyst and ametrine (Balitsky et al., 1970; Balitsky, 1980). The diagram further shows that there are conditions under which synthetic amethyst, citrine, or ametrine—as well as bi-colored amethyst-brown quartz and amethyst-green quartz—can be grown in acidic, neutral, or alkaline solutions.

Growth Rate and Coloration. The incorporation of iron impurities—and thus the development of the specific ametrine coloration—is dependent on the growth rate and surface structure of the different growth sectors (as explained by Balitsky and Balitskaya, 1986; see figure 3). The growth conditions must be closely regulated so that the amethyst- and citrine-forming iron impurities are captured simultaneously by different growth sectors in a crystal.

Commercial Growth and Irradiation Processes. The technology for synthesizing ametrine is similar to that for synthetic amethyst and synthetic citrine. The crystals are grown hydrothermally in concentrated alkaline (K_2CO_3) solutions at temperatures of 330°–370°C and pressures in the range of 1,200 to 1,500 atmospheres, in autoclaves ranging from 1,000 to 1,500 liters in volume (for photos of the factory, visit the Web site http://minerals.gps.caltech.edu/ametrine). The crushed silica used to grow the synthetic quartz is derived from natural or synthetic quartz with a very low aluminum content (10–100 ppm). To facilitate the incorporation of Fe^{3+} into the growing crystal structure, manganese nitrate, $Mn(NO_3)_2$, is used as an oxidizer.

The synthetic ametrine crystals are grown on seeds, prepared from colorless synthetic quartz crystals, that have a specified crystallographic orientation, shape, and size. Two types of seeds are used to produce the tabular synthetic ametrine crystals: (1) seeds cut parallel to the positive and negative rhombohedra; and, more commonly, (2) seeds cut parallel to the basal pinacoid. In both cases, the crystals are

grown at rates slightly below the critical rates (see figure 3) to produce the optimum distribution and intensity of color. The basal surfaces of crystals grown on seeds cut parallel to the basal pinacoid grow at about 0.8–1.0 mm/day. Rhombohedral faces, however, grow much slower (0.3–0.4 mm/day for the negative rhombohedral face, and 0.08–0.1 mm/day for the positive rhombohedral face). The rhombohedral *r* and *z* sectors are colorless or pale yellow as grown; subsequent gamma-ray irradiation, as described below, produces the purple color in these sectors (figure 4). The pinacoidal *c* sectors are yellow to orange as grown. Their primary citrine color is unaffected by the irradiation, although in a small proportion of crystals these sectors turn brownish orange due to the presence of a minor amethyst component.

Figure 3. The growth rate of synthetic ametrine strongly influences the coloration of the r *and* z *sectors (see figure 4 for an example of the coloration of the* r, z, *and* c *growth sectors). This schematic diagram shows the effect of growth rate on the capture and distribution of amethyst- and citrine-forming impurities in these two sectors. The color intensity is directly related to the quantity of captured iron impurities.* V^r_{cr} *and* V^z_{cr} *are the critical growth rates for the* r *and* z *faces, respectively (i.e., the growth rate at which the maximum color intensity will be produced). Above these critical values, the color intensity decreases, and the* r *and* z *sectors begin to capture citrine-forming impurities. In the diagram, the color of each line indicates the particular color-forming impurities that are incorporated into the* r *and* z *sectors at various growth rates. At higher growth rates, the* r *and* z *faces incorporate only citrine-forming impurities (i.e., in regions III, IV, and V for* r *and region V for* z*). To grow synthetic ametrine crystals with* r *and* z *sectors that will show an intense purple with irradiation, the growth is carefully maintained at just below the critical rate. The* c *faces capture only the citrine-forming impurities, regardless of the growth rate.*

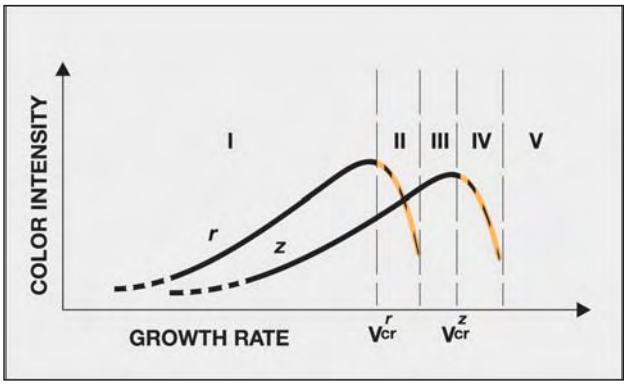

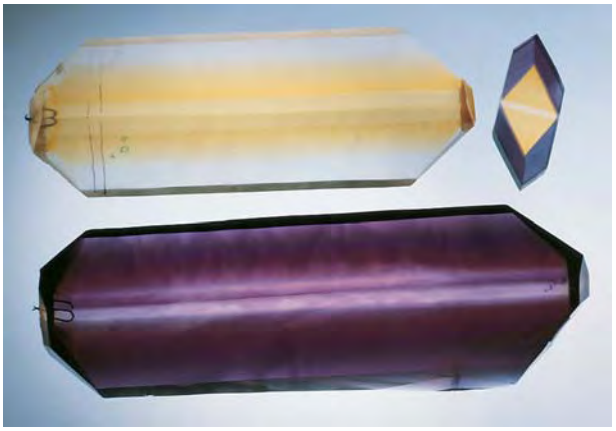

Figure 4. Commercially important synthetic ametrine is produced using rectangular seeds cut parallel to the basal pinacoid. The crystal on the upper left is shown before—and the crystal on the bottom (1.1 kg) after—gamma-ray irradiation. The slice on the upper right is a cross-section of an irradiated crystal; about 20 such slabs can be cut from a typical crystal. Within the slice, the colorless band is the seed plate, the yellow regions on either side of the seed are the c *sectors, and the dark purple zones are the* r *and* z *sectors (the* r *sectors are darker purple). Photo by Maha DeMaggio.*

By changing the shape, size, and orientation of the seed, and using other proprietary techniques, it is possible to grow synthetic ametrine crystals showing various habits, from tabular to prismatic (both symmetric and asymmetric), with a complex distribution of amethyst- and citrine-colored internal growth sectors. Most commercial production employs rectangular seed plates that are cut parallel to the basal pinacoid and elongated in the trigonal prism *x* [$11\bar{2}0$] direction (known as the ZX-cut). All of the synthetic ametrine samples examined for this study were grown using these seeds, which are typically 200–300 mm long, 20–50 mm wide, and 1.5–2.0 mm thick. Their use results in tabular crystals with the best color contrast between the different growth sectors. Very small quantities of crystals have been grown with the rectangular basal pinacoid seeds elongated in the hexagonal prism *m* [$10\bar{1}0$] direction (the ZY-cut), to get a more varied distribution of color.

To study the influence of seed orientation on the development of the synthetic amethyst and citrine portions, the Russian researchers are growing some crystals on seeds oriented at 15°–30° to the basal pinacoid face. Synthetic ametrine crystals with a

Figure 5. Each slab of synthetic ametrine typically yields 8–10 faceted samples. The largest faceted synthetic ametrine shown here weighs 20 ct. Photo by Maha DeMaggio.

prismatic morphology are also grown; they require special seeds and a proprietary morphology-controlling technique. Currently, these crystals are being produced for commercial use at a rate of only 2–3 kg per month. A detailed gemological study of this material is underway by the current authors.

The largest synthetic ametrine crystal grown thus far by the Russian authors weighed 4.5 kg. Crystals typically range from 0.45 to 1.2 kg, and measure 20 × 6 × 2 cm to 21 × 8 × 4 cm. For maximum amethyst color saturation, the crystals are irradiated with a cobalt-60 gamma-ray source for about three hours, resulting in a dose of about 5 Mrads. To fulfill customer requests, occasionally the crystals are heat treated (at 330°–350°C for one hour) to reduce the color intensity of the synthetic citrine portions.

Figure 6. These faceted synthetic ametrines (7.53–46.44 ct) represent some of the samples examined for this study. Photo by Maha DeMaggio.

CUTTING

The elongate, tabular crystals of synthetic ametrine are first cut perpendicular to their length into several slabs (see, e.g., figures 4 and 5). A 200-mm-long tabular crystal typically yields 20 slabs. The slabs contain both amethyst- and citrine-colored portions, except for those cut from near the ends of the crystals. Each slab yields about 8–10 faceted gems with an average weight of 10–15 ct (see, e.g., figure 5), although gems exceeding 50 ct can be cut. Some of the faceted gems will be almost entirely purple or yellow, depending on the portion of the slab from which they were cut. Rectangular, cushion, and oval shapes are most common.

Approximately 180 faceted stones are obtained from a typical rough crystal, for an overall yield of about 50%. No noticeable differences in physical properties, such as brittleness and hardness, have been reported for synthetic and natural ametrine during cutting and polishing.

MATERIALS AND METHODS

All of the synthetic ametrine samples included in this study were grown on tabular ZX-cut seeds. About 300 synthetic ametrine crystals (80 × 20 × 10 mm to 250 × 80 × 50 mm) and 150 faceted gems (1–40 ct) were examined by the Russian authors and their staff. The GIA and Caltech authors studied seven crystals, six polished crystal fragments, and 10 faceted samples of synthetic ametrine. The largest crystal studied at GIA measured 207.1 × 64.5 × 30.2 mm and weighed 1.1 kg. The faceted samples examined at GIA were cut in oval and various fancy shapes, and ranged from 7.53 ct to 46.44 ct (figure 6). To explore the dependence of physical and gemological properties on crystallographic orientation, we had 12 rough samples cut and polished in specific orientations (e.g., parallel and perpendicular to the optic axis). The resulting slabs weighed 10.30–65.80 ct and were studied by authors from all three institutions.

In addition, the GIA and Caltech researchers documented the gemological properties of the following samples of natural ametrine from the Anahí mine: seven crystals (50–56 grams), three slabs cut parallel to the optic axis (25.88–48.55 ct), three slabs

cut perpendicular to the optic axis (26.00–168.90 ct), and 30 faceted samples (3.90 ct–140.39 ct; see, e.g., figure 7) in various shapes.

Standard gem-testing equipment and methods were used to characterize all 40 of the faceted samples examined at GIA. The equipment included: a GIA GEM Duplex II refractometer with a near-monochromatic, sodium-equivalent light source; a polariscope, a calcite dichroscope, a Chelsea color filter, a GIA GEM combination long- and short-wave ultraviolet lamp unit (4 watts), a Beck desk-model prism spectroscope mounted on an illumination base, and a binocular gemological microscope. Twinning was observed with an immersion cell and cross-polarized light, at 7×–45× magnification. Specific gravity values were hydrostatically determined for three synthetic and five natural samples using a Mettler AM100 electronic balance.

Absorption spectra in the ultraviolet-visible-near infrared (UV-Vis-NIR) were obtained at GIA with two instruments (a Hitachi U-4001 and a Pye-Unicam 8800) for some of the natural ametrine (two crystals, three slabs, and 15 faceted stones) and synthetic ametrine (five crystals, three slabs, and 10 faceted samples). UV-Vis-NIR absorption spectra were also collected at Caltech, with a diode array microspectrometer. Four slabs and one cube of natural ametrine, and four slabs of synthetic ametrine, were chosen for detailed study on this system. Infrared spectra were recorded at GIA (on the same samples as for UV-Vis-NIR spectroscopy) with a Nicolet Magna-550 spectrophotometer, and at Caltech (four slabs each of natural and synthetic ametrine) with a Nicolet 860 instrument. Additional data for 20 crystals, 30 slabs, and 20 faceted synthetic ametrine samples were collected by the Russian authors using a SPECORD M40 spectrometer (visible range) and a Perkin-Elmer 983 spectrophotometer (infrared range). Equivalent instruments at the three locations gave comparable results.

Qualitative chemical analyses of 15 natural and 15 synthetic ametrine samples were obtained at GIA by energy-dispersive X-ray fluorescence (EDXRF) spectrometry, using a Tracor-Northern Spectrace TN 5000 instrument. Semi-quantitative chemical analyses of five natural (two slabs, three faceted) and four synthetic (two slabs, two faceted) ametrine samples were also performed at Caltech, using a Kevex-IXRF 7000 system in conjunction with the Fundamental Parameters program (supplied with the instrument's software) and silica-metal oxide mixtures as confirmatory standards.

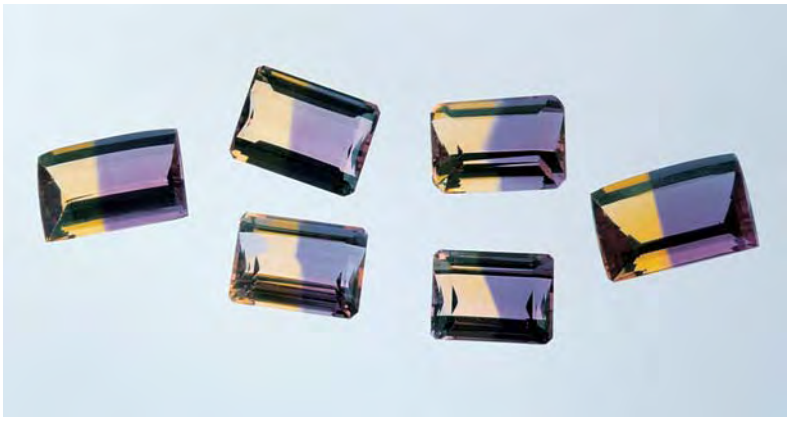

Figure 7. Natural ametrine was obtained for comparison with the synthetic material. The largest faceted ametrine shown here weighs 21.93 ct. Photo by Maha DeMaggio.

Raman spectra were collected using a Renishaw 2000 laser Raman microspectrometer at GIA on 10 natural and 10 synthetic faceted samples. Each was analyzed in both the citrine and amethyst regions without any change in the orientation of the sample. In addition, Raman spectra of doubly polished slabs of both natural and synthetic ametrine were obtained at Caltech using a Kaiser Optics Holoprobe instrument with an EIC probe head. Because the initial results obtained by both instruments suggested that Raman spectra were not particularly useful for identification purposes, a comprehensive Raman study was not undertaken.

To evaluate the color stability of the synthetic ametrine, the Russian authors heated 30 rough crystals, 20 slabs, and 50 crystal fragments in air, at temperatures up to 700°C. After the amethyst color faded in a particular temperature range, the faded samples were re-irradiated with gamma rays to investigate color restoration.

RESULTS AND DISCUSSION

Morphology of Natural and Synthetic Ametrine. As seen in most natural amethyst, natural ametrine crystals typically have a prismatic habit, elongated parallel to the optic axis (c-axis), and are terminated by the rhombohedral faces *r* $\{10\bar{1}1\}$ and *z* $\{01\bar{1}1\}$ (figure 8). In some crystals, both of these rhombohedra are equally developed, so that the terminations resemble hexagonal pyramids; a small, rough *c* (0001) face is occasionally present (Vasconcelos et al., 1994). Prism faces *m* $\{10\bar{1}0\}$ are commonly developed, and are striated at right angles to the c-axis. Rarely, other faces are developed, such as the trigonal prism *x* $\{11\bar{2}0\}$ and trigonal dipyramid *s* $\{11\bar{2}1\}$; if present, they are very small.

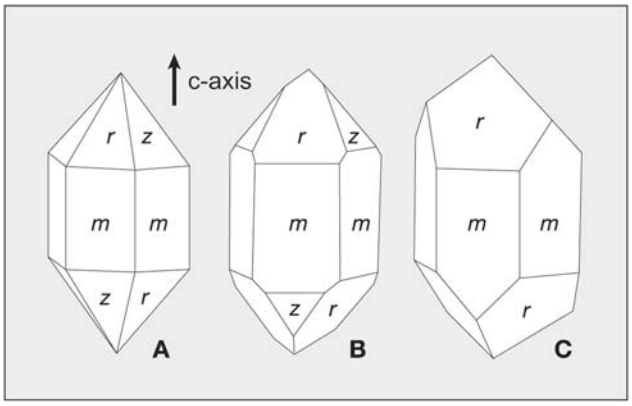

*Figure 8. Natural quartz crystals commonly show a simple arrangement of prism (*m*) and rhombohedral (*r *and* z*) faces. Ametrine crystals are typically prismatic, and are terminated by* r *and* z *faces of variable size. In natural ametrine crystal A, the rhombohedral faces are equally developed, so that the terminations resemble hexagonal pyramids. In most ametrine crystals, however, the terminations resemble those shown by B and C.*

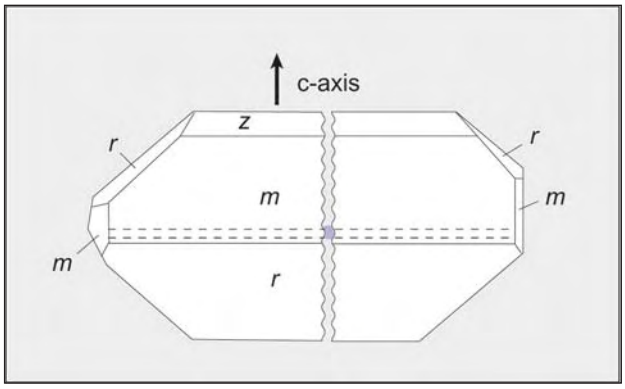

Figure 9. This schematic diagram illustrates a synthetic ametrine crystal that has been grown on a ZX-cut seed. The crystal is elongated along the seed (indicated here by dashed lines), and is bounded by r, z, m, *and* +x *faces. The* +x *faces are not visible in this diagram, because they are located on the back of the crystal, behind the* m *faces.*

Unlike natural ametrine, synthetic ametrine crystals are usually tabular, because a seed plate is used to start the growth. As noted earlier, the crystal morphology varies depending on the characteristics of the seed plate and the growth conditions. The crystals we examined for this study, all grown on ZX-cut seeds, were bounded mainly by *m* and *r* faces (figure 9); *z* faces were smaller, and the *+x* and *–x* faces were seldom present. A short steel wire—used to suspend the seed plate in the autoclave—was usually present at one end of the crystals.

Color and Color Distribution. The color distribution and internal features of the synthetic ametrine crystals are best seen when the they are sliced parallel to the *x* and *m* faces (figure 10). As noted earlier, the *c* sectors are synthetic citrine (orangy yellow to moderate orange), and the *r* and *z* sectors are synthetic amethyst (moderate to strong purple). The purple coloration is somewhat more intense in the *r* sectors than the *z* sectors. The samples exhibited moderate dichroism (violet purple to violet) in the amethyst-colored portion, and very weak to weak dichroism (orangy yellow to orange) in the citrine-colored portion.

In the synthetic ametrine samples we examined, the synthetic citrine portions were often more intensely colored than those in natural ametrine of similar thickness (see, e.g., figure 1). In general, we observed that the synthetic amethyst portions in

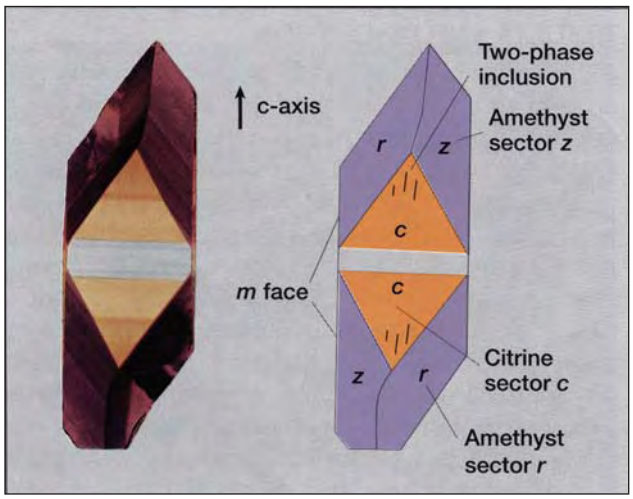

Figure 10. Several internal features in synthetic ametrine grown on tabular ZX-cut seeds are visible in this slab (6.0 cm long) and the corresponding schematic diagram. The slab was sliced parallel to the x *faces; it shows amethyst coloration in the* r *and* z *sectors, and citrine coloration in the c sectors. Color zoning is present in both the synthetic citrine and amethyst regions, and faint streaks consisting of liquid-gas inclusions are elongated parallel to the optic axis in the citrine region. The citrine color zoning is oriented parallel to the colorless seed (and perpendicular to the optic axis), and the amethyst color zoning is oriented parallel to the rhombohedral crystal faces. Photo by Maha DeMaggio.*

our samples were also more intensely colored than their natural amethyst counterparts.

The amethyst-citrine color boundary in synthetic ametrine (i.e., the boundary between the *c* sectors and the adjacent *r* and/or *z* sectors) is oriented roughly parallel to the rhombohedral faces, or at about 51° to the optic axis for *r* sector amethyst and 23° to the optic axis for *z* sector amethyst. In contrast, the color boundary in natural ametrine (i.e., the boundary between the amethyst *r* sectors and the citrine *z* sectors) is oriented roughly parallel to the optic axis.

In addition, to obtain maximum cutting yield from the slabs, some synthetic stones may show a sharp bend or angle in the amethyst-citrine color boundary (see, e.g., figure 5). This angle varied from 22°–48° in the synthetic slabs and faceted samples examined at GIA. When natural ametrine is faceted to show the maximum color contrast between amethyst and citrine, the color boundary is usually straight (see, e.g., figure 7).

Color Stability. The citrine color in the synthetic ametrine remained stable during heating (at temperatures up to 700°C). The amethyst color was stable below 400°C. In the temperature range of 400°–450°C, the purple faded completely within two hours of exposure, but it was fully restored by subsequent gamma-ray irradiation. However, when the synthetic ametrine samples were heated to higher temperatures, especially above the α–β phase transformation of quartz at 573°C, the amethyst color centers in nearly all samples were destroyed irreversibly (i.e., the purple could not be restored with gamma-ray irradiation), and a milky turbidity obscured the color and transparency of both the amethyst and citrine zones. As the temperature was increased from 550° to 700°C, in particular, the intensity of milkiness increased, cracks appeared, and the orange component of the citrine color decreased.

Microscopic Characteristics. Amethyst and citrine color zoning, stream-like structures, polysynthetic Brazil-law twinning, and two-phase (liquid-gas) inclusions were the principal microscopic features seen in the synthetic ametrine. The slab in figure 10 shows most of these features, and the corresponding schematic diagram illustrates their interrelationships and their orientation relative to the optic axis.

The citrine portions (*c* sectors) of the faceted synthetic ametrine commonly showed color zoning, oriented perpendicular to the optic axis. In the amethyst portion (*r* and *z* sectors), color zoning was generally observed, and was always oriented parallel to either the *r* or the *z* crystal faces, or at about 50° to the optic axis. Rarely, stream-like structures were observed in the synthetic citrine portions. With oblique lighting, these appeared as wavy stripes of color (figure 11) that were subparallel to the optic axis. They result from surface irregularities caused by growth hillocks on the basal pinacoid as the crystal grew.

Figure 11. Stream-like structures are visible in the citrine portion of this 4.25 ct faceted synthetic ametrine. Photo by Taijin Lu.

No twinning was observed in the citrine portion of the faceted synthetic ametrine. Brazil twins (see, e.g., figure 12, left) were observed by the Russian authors in the synthetic amethyst *r* sectors of only a few of the 150 faceted samples. As observed with crossed polarizers, Brazil twins in the synthetic amethyst portions formed a distinctive polysynthetic twinning pattern: a group of straight, thin, parallel lamellae showing various interference colors. In contrast, the amethyst sectors in all of the natural ametrine studied showed Brazil twinning. Brazil twin boundaries in natural amethyst show distinctive curved or mottled patterns that are sometimes accompanied by linear areas of extinction called Brewster fringes (Brewster, 1823; Crowningshield et al., 1986; Lu and Sunagawa, 1990; Vasconcelos et al., 1994; see figure 12, center and right). Brewster fringes were not observed in the synthetic ametrine.

Two-phase (liquid-gas) inclusions were observed only rarely in the synthetic citrine portions (figure 13), and very rarely in the synthetic amethyst portions. These inclusions were oval or needle shaped, and were elongated parallel to the optic axis and the stream-like structures; in a few instances, they were visible to the unaided eye with strong light.

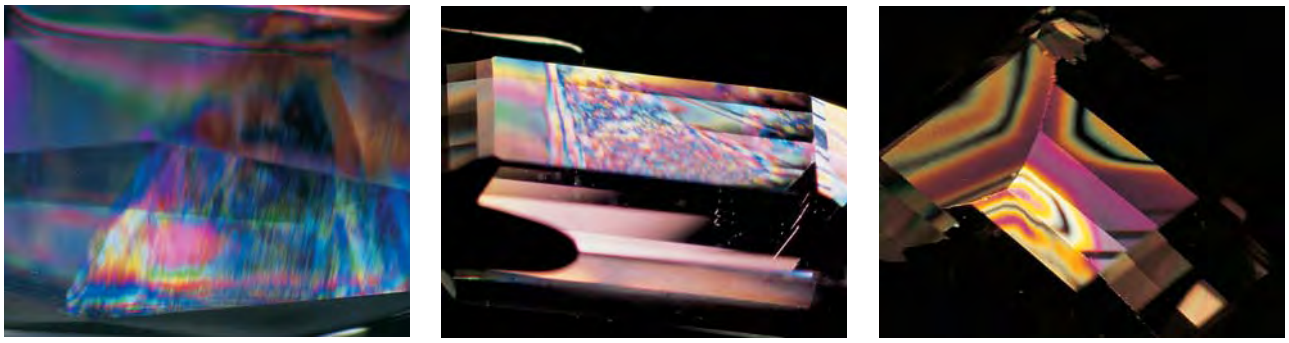

Figure 12. Brazil twins were observed only rarely in the amethyst portion of the faceted synthetic ametrines. They were composed of polysynthetic twin lamellae (thin, straight parallel lamellae showing various interference colors), as shown in the 12.42 ct faceted synthetic amethyst on the left (photomicrograph by John I. Koivula, magnified 15×). In contrast, the Brazil twins in the amethyst portion of the 11.47 ct natural ametrine in the center (photomicrograph by Taijin Lu) form complex curved patterns; the citrine portion is demarcated by the untwinned area on the far left side of the stone. Although the twinning in these two examples appears somewhat similar, the striated appearance of the twinning in the synthetic sample is diagnostic. Some natural samples show distinctive curved "classic" Brazil twins that may be accompanied by the darker Brewster fringes, as shown by the amethyst on the far right (photomicrograph by Shane McClure).

Occasionally, small dark brown-to-black particles were seen, sometimes with a needle-like morphology, along the interface between the seed plate and the citrine portions of the synthetic ametrine. Although they were not identified, the growth conditions suggest that they could be hydrous Fe-oxides or Mn-oxides.

According to J. Koivula (pers. comm., 1999), other primary fluid inclusions showing a flattened morphology are occasionally observed along the synthetic amethyst-citrine color boundaries. Such inclusions have also been noted along the length of the seed plate interface, and near the location of the wire used to suspend the crystals during growth. Both the synthetic amethyst and citrine portions also may have partially healed fractures composed of numerous tiny voids containing both liquid and gas phases. Unlike some of the primary fluid inclusions described above, these secondary fingerprint-like fluid inclusions are not oriented in any specific direction.

Figure 13. Needle-like two phase (liquid-gas) inclusions were seen only rarely in the citrine portion of the synthetic ametrines. The inclusions are elongated parallel to the optic axis. Photo by Taijin Lu; magnified 10×.

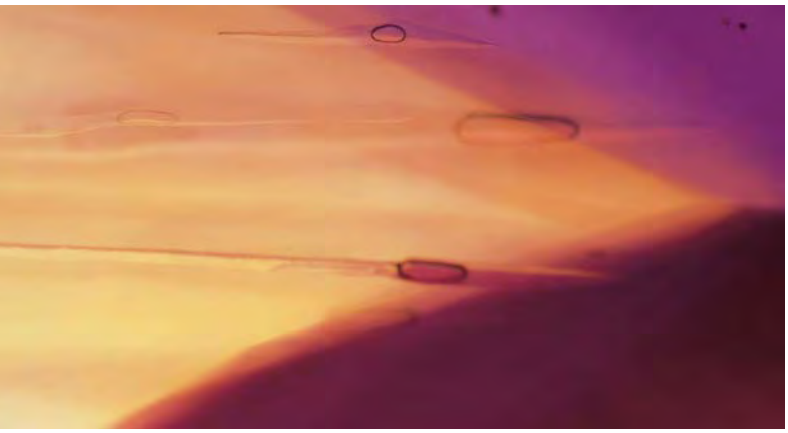

Spectroscopic Features. The absorption spectra in the UV-Vis-NIR regions were identical for natural and synthetic ametrine. In the amethyst portions of both types of ametrine, we saw characteristic absorption bands at 270, 350, 540, and 930 nm. In the citrine portions, an absorption edge rose abruptly in the 400–500 nm range, and showed weak bands superimposed at 540 and 930 nm.

Although the infrared spectra of the natural and synthetic ametrines were similar, we noted some distinctive differences. The synthetic citrine portions showed a broad, strong region of absorption from about 3700 to 2500 cm^{-1} (figure 14A), which is due to water. A similar broad band occurs in the citrine portion of natural ametrine (Vasconcelos et al., 1994), but it is much weaker. Weak OH^- peaks are superimposed on the broad band in the 3700–3500 cm^{-1} region of both materials, but the natural citrine has a weak peak at 3595 cm^{-1}, which is not seen in the synthetic material (figure 14B). In addition, one dark sample of synthetic ametrine showed weak peaks at 3555 and 3528 cm^{-1} in the citrine portion.

The infrared spectra of the amethyst zones in both the synthetic and natural ametrine show more

intense OH^- peaks, superimposed on a broad absorption band at 3435 cm^{-1} (figure 14C). The main distinction between the synthetic and natural amethyst portions is a weak band in most of the synthetic amethyst at 3543 cm^{-1} (figure 14D). Other differences, such as a weak band at 3595 cm^{-1} in the natural material, are probably too subtle to use for identification purposes.

The Raman spectra of synthetic ametrine are typical for quartz. When a comparison of the spectra of oriented samples was made for the different color zones in natural and synthetic ametrine, there was only a very slight difference: A weak 1046 cm^{-1} peak observed in both natural and synthetic ametrine was somewhat weaker in the natural ametrine.

Chemical Analyses. Qualitative EDXRF spectra of the synthetic ametrine showed the presence of iron (Fe, all 15 samples) potassium (K, 12 samples), manganese (Mn, 12 samples), and zinc (Zn, 11 samples) as trace elements. In general, higher concentrations of these elements were present in the citrine zones than in the amethyst zones. Traces of nickel (Ni) and chromium (Cr) were also observed in the citrine and amethyst portions, respectively, of single synthetic samples. We were not surprised to find these elements, since Fe is the chromophore, K and Mn are used in the growth process, and Ni, Cr, and Zn are components of the steel used in the autoclaves.

Semi-quantitative EDXRF analyses of two slabs of synthetic ametrine revealed large variations in

Figure 14. Some differences were noted in the mid-infrared spectra of the natural and synthetic ametrine. Compared to natural material, the synthetic citrine zones exhibit a more intense, broad absorption band in the 3700–2500 cm^{-1} region (A); weak peaks at 3555 and 3528 cm^{-1} were diagnostic features in one darker synthetic citrine section (B). The spectra of the amethyst zones in both synthetic and natural ametrine are similar (C), but a weak 3543 cm^{-1} peak is usually seen in the synthetic material (D). The spectra are presented normalized to 1.0 mm thickness.

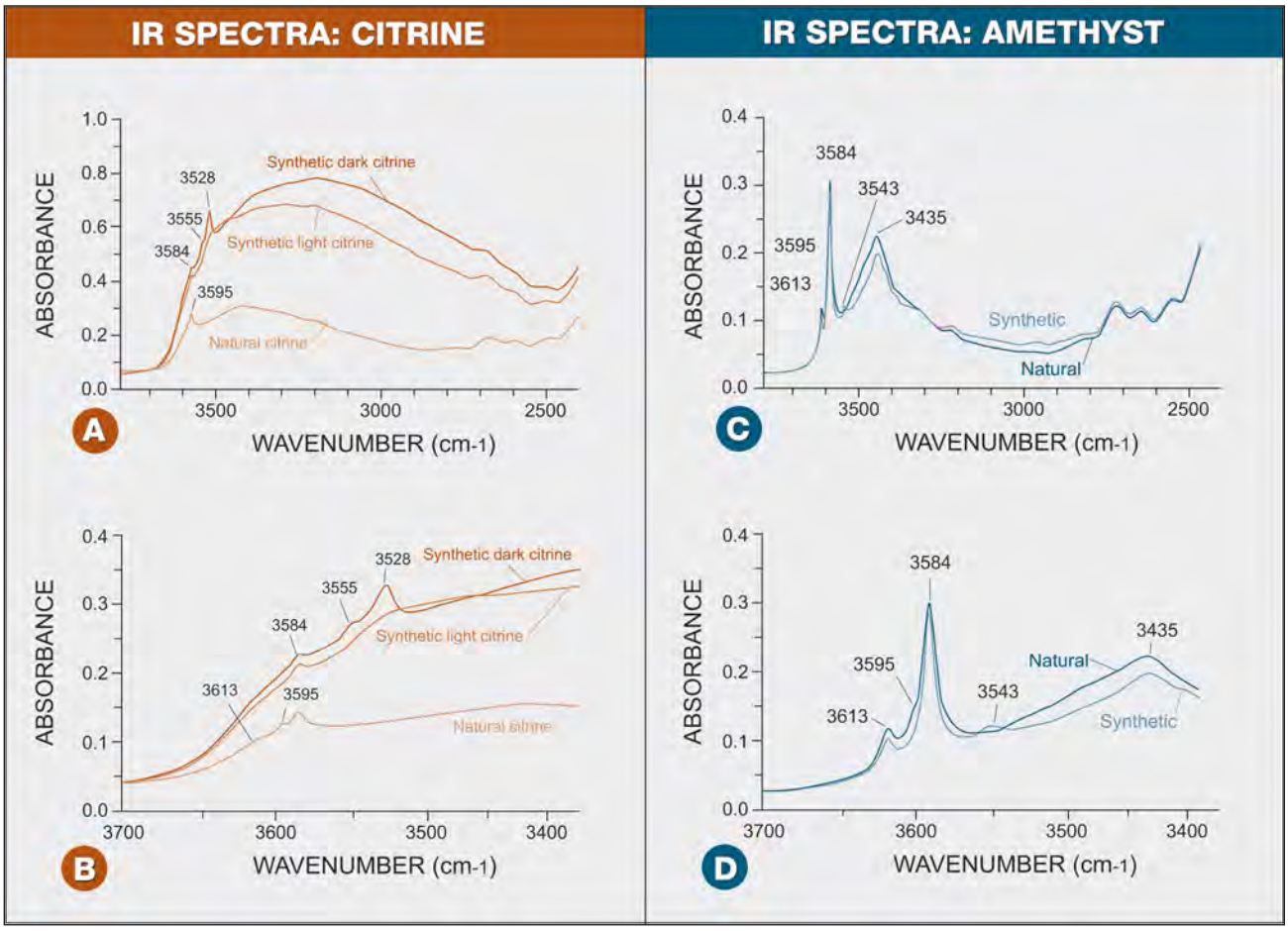

the concentrations of the above-mentioned trace elements which could be correlated to the amount of inclusions present. The two faceted samples analyzed, which were eye-clean, had lower impurity contents and showed less-pronounced chemical variations.

The quantitative (electron microprobe) analyses of natural ametrine reported by Vasconcelos et al. (1994) showed higher concentrations of iron (68–125 ppm) in the citrine zones than in the amethyst zones (19–40 ppm); data for other trace elements were not reported. In our samples of natural ametrine, we detected traces of Fe, Zn, K, Mn, and Al. The semi-quantitative data we obtained provided only relative amounts of the elements detected, so we compared the concentrations of K, Mn, Fe, and Zn in both natural and synthetic ametrine by normalizing the raw data to 1000 silicon counts per second. We found that the synthetic ametrine had higher contents of Zn (×2), Fe (×2 to ×3), Mn (×4 to ×6), and K (×4) than the natural ametrine; aluminum was present at similar (low) levels in both materials. It appears that a combination of higher K, Mn, Fe, and Zn is a distinctive feature of synthetic ametrine.

SEPARATING NATURAL FROM SYNTHETIC AMETRINE

Table 1 compares some distinguishing properties of natural ametrine and the Russian synthetic ametrine grown on tabular ZX-cut seeds. Note that R.I., birefringence, S.G., UV fluorescence, and UV-Vis-NIR absorption spectra were identical in the natural and synthetic samples.

Separating the crystals is straightforward, since their morphology is distinctive. Natural ametrine usually forms as prismatic crystals with well-developed rhombohedral faces, whereas the commercially important synthetic ametrine crystals display a tabular habit bounded mainly by *m* and *r* faces. The synthetic crystals also commonly contain a short steel wire at one of the end.

Faceted stones are more difficult to distinguish, but a number of properties provide indications:

1. The citrine color in synthetic ametrine may span a wide range, from pale yellow to moderate orange. In the synthetic samples we studied, the citrine portions were often more intensely colored than those in natural ametrine of similar thickness (again, see figure 1). The amethyst portions of our samples were also more intensely colored than those in natural ametrine of similar thickness.
2. Faceted natural ametrine commonly displays a sharp, straight boundary between the citrine and amethyst portions. Synthetic ametrine, especially when cut in fancy shapes, sometimes displays a sharp bend in the color boundary (angles of 22°–48° were measured in the GIA samples). While the amethyst-citrine color boundary in the synthetic ametrine examined for this study is oriented roughly parallel to the rhombohedral faces (or at about 51° to the optic axis for *r* sector amethyst and 23° to the optic axis for *z* sector amethyst), in natural ametrine it is oriented roughly parallel to the optic axis.
3. The crystallographic orientations of the color zones and the rare stream-like structures in the synthetic citrine portions are distinctive. The color zones are oriented perpendicular to the optic axis, and the stream-like structures are oriented parallel to the optic axis. We recommend using cross-polarized light to locate the optic axis in faceted samples, in order to provide a reference for checking the orientation of color zones and stream-like structures. In natural ametrine, the color zoning in both the amethyst and citrine portions is oriented parallel to the rhombohedral faces, and the bands usually are spaced irregularly.
4. In the amethyst portions of natural ametrine, Brazil-law twinning is almost always present, and Brewster fringes are often observed. However, Brazil twinning was seen only rarely in the amethyst portions of synthetic ametrine, in the form of subtle parallel twin lamellae. Due to the variety in forms and patterns displayed by Brazil twinning in both natural and synthetic amethyst (see, e.g., Koivula and Fritsch, 1989), this feature should not be used alone to identify a stone as synthetic. However, if a sample does show the "ideal" curved Brazil twins with Brewster fringes (again, see figure 12, right), it can be identified as natural.
5. Irregular planes of two-phase (liquid-gas) inclusions are commonly observed in both color portions of natural ametrine (Vasconcelos et al., 1994). In synthetic ametrine, elongate two-phase (liquid-gas) inclusions were seen only rarely. However, these inclusions would be diagnostic

only for those who are very experienced with quartz inclusions.

6. Natural and synthetic ametrine can usually be separated by their infrared spectra. The synthetic citrine portion has more intense absorption in the 3700–2500 cm^{-1} range of the infrared spectrum, and weak peaks at 3555 and 3528 cm^{-1} in dark material may be diagnostic. The synthetic amethyst showed a weak band at 3543 cm^{-1} that has not been observed in the natural amethyst portions.
7. As determined by EDXRF chemical analysis, synthetic ametrine will typically show higher contents of K, Mn, Fe, and Zn than occur in natural ametrine.

Even with advanced testing, the identification of natural and synthetic ametrine should rely on multiple criteria, since some of the distinguishing characteristics may be absent, and some features overlap. Positive identification may not be possible in all cases.

CONCLUSIONS

By 1994, the technology was available to produce synthetic ametrine commercially. To date, several hundred kilograms of this material have been grown and are being distributed in the jewelry marketplace.

Although there are many similarities between natural ametrine and the hydrothermal synthetic ametrine grown in Russia that was examined for this study, most faceted samples can be separated by a combination of standard gemological methods, especially by observation of internal features such as color zoning and twinning. Advanced techniques

TABLE 1. Distinguishing properties of natural ametrine and the Russian synthetic ametrine obtained for this study.[a]

Property	Synthetic	Natural
Crystal morphology	Tabular habit, normally elongated in the trigonal prism *x* direction. Prism *m* and rhombohedral *r* faces are the best developed. Seed plate is oriented perpendicular to the c-axis.	Prismatic habit consisting of rhombohedral faces *r* and *z*, and prism faces *m*.
Color	*Amethyst portion:* moderate to strong purple in the *r* and *z* sectors. *Citrine portion:* orangy yellow to orange in the *c* sectors. Typically more intensely colored than natural ametrine in both portions.	*Amethyst portion:* pale purple to intense violet-purple in *r* sectors. *Citrine portion:* light yellow to orange-yellow in *z* sectors.
Color boundary	Usually a sharp straight boundary, oriented at 51° or 23° to the optic axis for the *r* and *z* sectors, respectively; may show a sharp bend.	Usually a sharp straight boundary, oriented parallel to the optic axis.
Growth and color zoning	*Amethyst portion:* color zoning oriented parallel to the *r* or *z* crystal faces, or at about 50° to the optic axis. *Citrine portion:* color zoning oriented parallel parallel to the seed plate, or perpendicular to the optic axis; rarely, stream-like structures observed subparallel to the optic axis.	Color zoning in both the amethyst and citrine portions oriented parallel to the rhombohedral faces.
Twinning	Polysynthetic Brazil twins are observed very rarely in the amethyst portion. No twins in the citrine portion.	Brazil twins (sometimes with Brewster fringes) in the amethyst portion, typically with distinctive curved or mottled patterns. No twins in the citrine portion.
Inclusions	Rare two-phase (liquid-gas) inclusions in the citrine portion, elongated parallel to the optic axis.	Irregular planes of two-phase inclusions often observed along cracks in both portions.
IR absorption spectrum	*Amethyst portion:* usually a weak peak at 3543 cm^{-1}. *Citrine portion:* a more intense, broad absorption in the 3700–2500 cm^{-1} region; weak peaks at 3555 and 3528 cm^{-1} present in one darker sample.	*Amethyst portion:* no peak at 3543 cm^{-1}. *Citrine portion:* weaker broad absorption in the 3700–2500 cm^{-1} region; no 3528 cm^{-1} peak.
Trace elements detected by EDXRF	K, Mn, Fe, and Zn significantly higher than in natural samples; also traces of Al detected.	Fe and Zn; K, Mn, and Al detected in some samples at low concentrations.

[a]*Both materials share the following properties: R.I.—nw=1.540–1.541, ne=1.550; birefringence—0.009–0.010; S.G.—2.65; UV fluorescence—Inert to both short- and long-wave UV; UV-Vis-NIR absorption spectrum—amethyst portion: bands at 270, 350, 540,and 930 nm; citrine portion: very strong absorption at 400–500 nm and weak lines at 540 and 930 nm.*

(infrared spectroscopy and EDXRF analysis) can provide further useful data for the separation of these two materials. Note, however, that the diagnostic features presented here are specific to ametrine and are not necessarily applicable to either amethyst or citrine in general.

It must also be noted that the technology of synthetic crystal growth is constantly evolving. Prismatic synthetic ametrine crystals are now being commercially produced, and these are very similar in crystal morphology and color distribution to natural ametrine. It is, therefore, especially important that the gemologist continue to use a multitude of tests to make a conclusive identification.

Acknowledgments: The authors thank Dr. Ilene Reinitz, John Koivula, Shane McClure, and Dr. Mary Johnson of the GIA Gem Trade Laboratory for their useful comments on the manuscript, and Julia Goreva of Caltech for her assistance with the translation of technical articles from Russian to English. Funding for research at Caltech was provided by the White Rose Foundation. Funding for research in Russia was provided by the Russian Basic Research Foundation (grant # 97-05-64805).

REFERENCES

Balakirev V.G., Keivlenko E.Y., Nikolskaya L.V., Samoilovich M.I., Khadzhi V.E., Tsinober L.I. (1979) *Mineralogy and Crystal Physics of Gem Varieties of Silica*. Nedra Publishers, Moscow. [in Russian].

Balitsky V.S. (1980) Synthetic amethyst: Its history, methods of growing, morphology and peculiar features. *Zeitschrift der Deutschen Gemmologischen Gesellschaft*, Vol. 29, No. 1, pp. 5–16.

Balitsky V.S., Khetchikov L.N., Dorogovin B.A. (1970) Some specific geochemical conditions of amethyst formation. In V.P. Butusov, Ed., *Trudy VNIISIMS, Synthesis and Experimental Investigation*, Vol. 13, Nedra Publishers, Moscow, pp. 75–82 [in Russian].

Balitsky V.S., Lisitsina E.E. (1981) *Synthetic Analogues and Imitations of Natural Gemstones*. Nedra Publishers, Moscow [in Russian].

Balitsky V.S., Balitskaya O.V. (1986) The amethyst-citrine dichromatism in quartz and its origin. *Physics and Chemistry of Minerals*, Vol. 13, pp. 415–421.

Brewster D. (1823) On circular polarization, as exhibited in the optical structure of the amethyst, with remarks on the distribution of the coloring matter in that mineral. *Transactions of the Royal Society of Edinburgh*, Vol. 9, pp. 139–152.

Crowningshield R., Hurlbut C., Fryer C.W. (1986) A simple procedure to separate natural from synthetic amethyst on the basis of twinning. *Gems & Gemology*, Vol. 22, No. 3, pp. 130–139.

Garrels R.M., Christ C.L. (1965) *Solutions, Minerals and Equilibria*. Freeman, Cooper & Co., San Francisco, CA, 450 pp.

Hehar W.C. (1980) The discovery of golden amethyst. *Lapidary Journal*, Vol. 34, pp. 582–583.

Hutton D.R. (1964) Paramagnetic resonance of Fe^{3+} in amethyst and citrine quartz. *Physics Letters*, Vol. 4, pp. 310–311.

Jones B. (1993) Is ametrine for real? *Rock & Gem*, Vol. 23, No. 9, pp. 46–52.

Koivula J.I. (1980) Citrine-amethyst quartz. *Gems & Gemology*, Vol. 16, No. 9, pp. 290–293.

Koivula J.I., Fritsch E. (1989) The growth of Brazil-twinned synthetic quartz and the potential for synthetic amethyst twinned on the Brazil law. *Gems & Gemology*, Vol. 25, No. 3, pp. 159–164.

Lehmann G. (1975) On the color centers of iron in amethyst and synthetic quartz: A discussion. *American Mineralogist*, Vol. 60, No. 3–4, pp. 335–337.

Lu T., Sunagawa I. (1990) Structure of Brazil twin boundaries in amethyst showing Brewster fringes. *Physics and Chemistry of Minerals*, Vol. 17, pp. 207–211.

Melnik Y.P., Drozdovskaya A.A., Vorobeva K.A. (1974) Physicochemical analysis of the dissolution, migration and deposition of iron in modern volcanic regions. In S. Naboko, Ed., *Modern Volcanic Systems*, Nauka publishers, Novosibirsk, pp. 119-126 [in Russian].

Nassau K. (1981) Artificially induced color in amethyst-citrine quartz. *Gems & Gemology*, Vol. 17, No. 1, pp. 37–39.

Rivero R. (1999) Synthetic ametrine and amethyst infiltrates Bolivian market. *ICA Gazette*, May/June/July issue, p. 15.

Rossman G.R. (1994) The colored varieties of silica. In P.J. Haney, Ed., *Silica, Reviews in Mineralogy*, Vol. 29, Mineralogical Society of America, Washington, DC, pp. 433–468.

Tsinober L.I., Chentsova L.G. (1959) Synthetic quartz with amethyst color. *Kristallografiya*, Vol. 4, pp. 633–635 [in Russian].

Vargas G., Vargas M. (1980) A new quartz gem material. *Lapidary Journal*, Vol. 34, No. 7, pp. 1504–1506.

Vasconcelos P., Wenk H.R., Rossman G.R. (1994) The Anahí ametrine mine, Bolivia. *Gems & Gemology*, Vol. 30, No. 1, pp. 4–23.

Zaitov M.M., Zaripov M.M., Samoilovich M.I. (1974) The Fe^{3+} EPR spectrum in irradiated quartz. *Kristallografiya*, Vol. 19, pp. 1090–1093 [in Russian].